[AMT10] Aqueous electrodeposition and properties of tin selenide thin films

Saravanan Nagalingam[1], Zulkarnain Zainal[1], Anuar Kassim[1], Mohd. Zobir Hussein[1], Wan Mahmood Mat Yunus[2]

[1]Department of Chemistry, [2]Department of Physics, Faculty of Science, Universiti Putra Malaysia, 43400 Serdang, Selangor, Malaysia

Introduction

Motivated by the potential applications of tin chalcogenides, investigations on these compounds are becoming particularly active in the field of materials chemistry. Tin chalcogenides offer a range of optical band gaps suitable for various optical and optoelectronic applications. These compounds are also used as sensor and laser materials, thin films polarizers and thermoelectric cooling materials (Zweibel, 2000). Considerable attention has been given by various researchers in studying the properties of tin selenide (SnSe). SnSe is a narrow band gap binary IV-VI semiconductor with an orthorhombic crystal structure. Among the uses of tin selenide (SnSe) are as memory switching devices, holographic recording systems, and infrared electronic devices (Lindgren *et al*., 2002). SnSe has been studied in the form of both single crystal and thin films (Subramanian *et al*., 1999; Yu *et al*., 1981; Agnithothri *et al*., 1979). SnSe could also be used in the fabrication of photoelectrochemical cells. The use of SnSe for this purpose could suppress photocorrosion and enhance the fill factor in electrical switches and in junction devices (Terada *et al*., 1971).

The methods used to prepare SnSe thin films are chemical bath deposition (Suguna *et al*., 1996), vacuum evaporation, chemical vapour deposition (Pramanik *et al*., 1988; Bennouna *et al*., 1983; Dang Tran, 1985) and electrodeposition (Subramanian *et al*., 1999; Engelken *et al*., 1986). Among these methods, electrodeposition is widely used because it is a simple, economical and viable technique, which produces films of good quality for device applications (Riveros *et al*., 2001; Pattabi *et al*., 2000). The attractive features of the method are the convenience for producing large area devices, low temperature growth, enable morphological, compositional and film thickness control by readily adjusting the electrical parameters, as well as the composition of the electrolytic solution (Riveros *et al*., 2001). We report here the electrodeposition of SnSe thin films under aqueous conditions in the presence of ethylendiaminetetraacetate (EDTA) as a chelating agent.

Materials and Methods

A conventional three-electrode cell was employed in this study. Ag/AgCl was used as the reference electrode to which all potentials were quoted. The working and counter electrodes were made from indium tin oxide (ITO) glass substrate and platinum, respectively. The ITO glass substrates were cleaned ultrasonically in ethanol and distilled water before the deposition process. The counter electrode was polished prior to the insertion into the electrolyte cell. EG & G Princeton Applied Research potentiostat driven by a software model 270 Electrochemical Analysis System was used to control the electrodeposition process and to monitor the current and voltage profiles. The electrolytes were prepared using analytical grade reagents and deionised water. Ethylendiaminetetraacetate (EDTA) was used to chelate with Sn^{2+} to obtain Sn-EDTA complex solution. The presence of EDTA in aqueous solution was found to improve the lifetime of the deposition bath as well as the adhesion of the deposited film on the substrate (Ghazali *et al.*, 1998). The deposition process was varied at various parameters such as solution temperature and deposition time. Effects of annealing in nitrogen (N_2) atmosphere towards the crystallinity of the material were also studied.

Prior to the deposition process, cyclic voltammetry (CV) test was run between -1.00 to 1.00 V on the cell containing the Sn-EDTA complex and disodium selenite (Na_2SeO_3) solution to probe the prospective potentials for deposition. The experiment was performed at room temperature (27 °C) under N_2 blanket

without stirring. The pH was maintained at 2.4 using HCl, which was added to prevent the formation of hydroxyl species and insoluble compounds (Ghazali *et al.*, 1998).

The films were deposited at various deposition potentials. Immediately after deposition, the deposits were tested for its durability by subjecting it to a steady stream of distilled water. The deposited films were kept for further comparison and analysis. X-ray diffraction (XRD) analysis was carried out using a Siemens D-5000 Diffractometer for the 2θ ranging from 2 - 60 ° with CuKα radiation (λ = 1.5418 Å). Scanning electron microscopy (SEM) was performed on a JEOL JSM 6400 Scanning Microscope. Optical absorption study was carried out using the Perkin Elmer UV/Vis Lambda 20 Spectrophotometer. The film-coated indium doped tin oxide (ITO) glass was placed across the sample radiation pathway while the uncoated ITO glass was put across the reference path. The raw data were manipulated for the determination of the band gap energy, E_g. Photoelectrochemical (PEC) experiment was performed in $K_3Fe(CN)_6/K_4Fe(CN)_6$ redox solution by running linear sweep voltammetry (LSV). A tungsten-halogen lamp (100 W) was used for illuminating the electrode.

Results and Discussion

The cyclic voltammogram of ITO glass electrode in the deposition bath containing mixture of Sn-EDTA and Na_2SeO_3 is shown in Figure 1. The current rise starts at about –0.40 V. This is due to the formation of SnSe compound on the surface of the electrode. The current increased as the potential was forwarded to more negative values. At higher potential values the deposition process is followed by the hydrogen evolution process, which is also reported to occur at higher negative potential values. However, no significance peak separation is observed that separates both the process. This suggests that the deposition process is best not to be proceeded at very negative values. During the reverse scan the current followed lower potential route, which is typical for deposition reaction. However no significance anodic peak is observed indicating that SnSe films formed during the reduction process is quite stable in the solution.

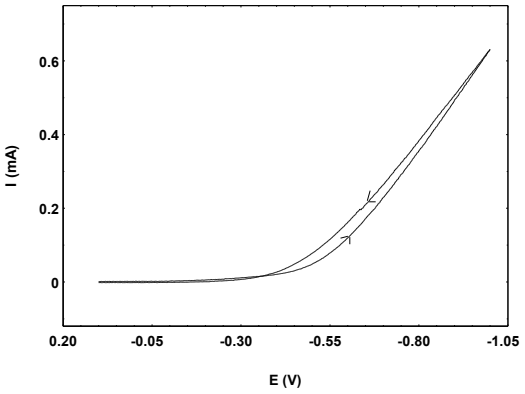

FIGURE 1 Cyclic voltammogram of ITO glass electrode in the deposition bath containing mixture of Sn-EDTA and Na_2SeO_3

The formation of SnSe follows according to reaction (1). Similar mechanisms have been proposed for the deposition of PbSe films (Saloniemi *et al.*, 1998).

$$Sn(EDTA)^{2-} + Se + 2H^+ + 2e^- \rightarrow SnSe + H_2EDTA^{2-} \quad (1)$$

Based on the CV result, significant deposition can be expected for potential above –0.40 V. Thus, deposition was carried out at potentials, -0.50, -0.60, -0.70, –0.80 and –0.90 V. Higher potential above –0.90 V was not attempted as this could lead to H_2 evolution reaction. Only the film deposited at –0.80 V at showed full surface coverage upon observation. However, the thickness of the film was very low indicating low amount of material deposited due to slow deposition rate. The following deposition process was carried out at 55 °C. The film deposited at this temperature covered the surface of the substrate completely with no pinhole effect. The appearance of the films was dark greyish in colour. Figure 2 shows the XRD plot of the film deposited at 55 °C. The peak at 2θ = 30.6 ° was most prominent corresponding to the (111) plane, which matched the orthorhombic SnSe phase (JCDPS File No: 32-1382). The SEM micrograph of the film deposited at 55 °C is shown in Figure 3. The micrograph of the film shows formation of somewhat thicker deposit which covers completely the surface of the substrate. Formation of granules, which was uniformly distributed over the deposit layer, could be observed. The sizes of these granules are quite similar and vary considerably from 2 μm to 4 μm.

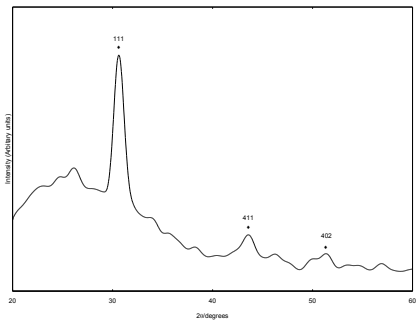

FIGURE 2 XRD plot of SnSe film deposited at 55 °C

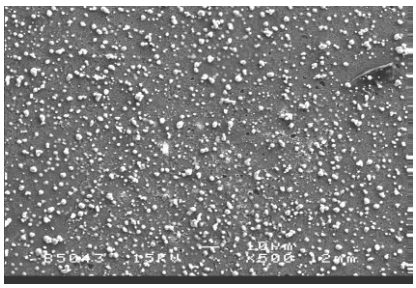

FIGURE 3 SEM micrograph of SnSe film prepared at 55 °C

Optical absorbance, A, versus the wavelength, λ, of the SnSe films prepared at 55 °C is shown in Figure 4. The film showed gradual absorption starting at 650 nm downward. Band gap energy and transition type was derived from mathematical treatment of the data obtained from the optical absorbance vs. wavelength with the following relationship for near-edge absorption:

$(Ah\nu)^{2/n} = k(h\nu - E_g)$

where ν is the frequency, h is the Planck's constant, k equals a constant while n carries the value of either 1 or 4. The bandgap, E_g, could be obtained from a straight line plot of $(Ahv)^{2/n}$ as a function of hν. Extrapolation of the line to the base line, where the value of $(Ahv)^{2/n}$ is zero, will give E_g. A linear trend is apparent where n in the relationship equals 4 (Figure 5). The straight-line behavior testifies an indirect transition of the band structure. The bandgap value obtained for the film prepared at 55 °C is about 1.08 eV, which matches the reported values of about 1 eV [Singh *et al.*, 1991; John *et al.*, 1994].

Figure 6 shows the XRD plot of the films deposited at different deposition time. The film deposited for 15 min shows only two peaks at 2θ = 30.5 and 31.3 ° corresponding to

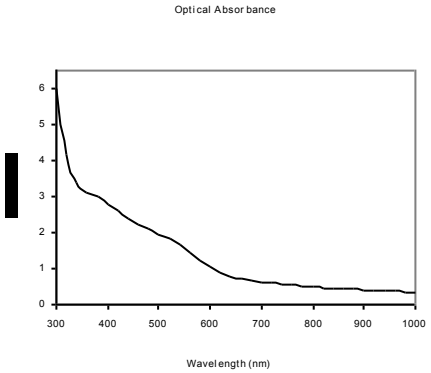

FIGURE 4 Optical absorbance vs. wavelength spectrum for SnSe film prepared at 55 ºC

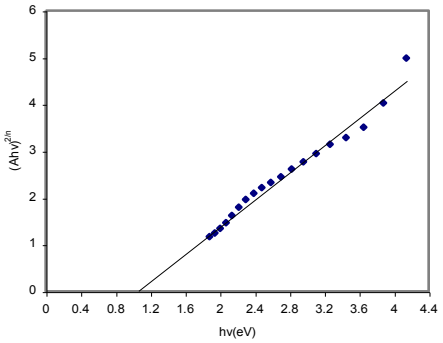

FIGURE 5 Plot of $(Ahv)^{2/n}$ vs. hν when n = 4 for SnSe film prepared at 55 °C

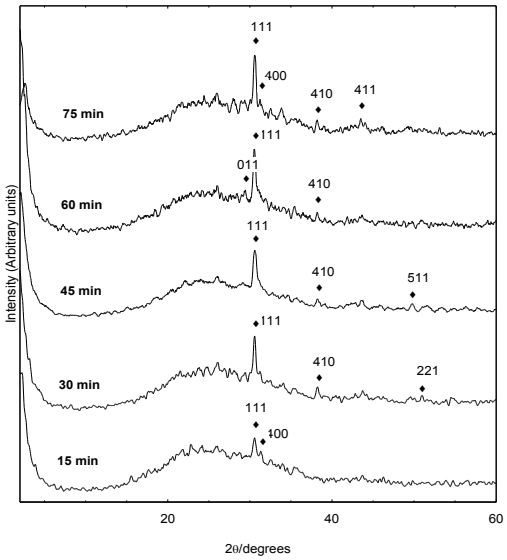

FIGURE 6 XRD data of samples prepared at various time

interplanar distances of 2.92 and 2.85 Å. These peaks are in well agreement to the JCPDS data for SnSe (File No.32-1382). As the deposition time was increased from 15 to 75 min the intensity of the peak that

correspond to (111) plane increased. This is accompanied by the appearance of four other peaks of SnSe at 2θ = 30.6, 31.3, 38.2 and 43.5 ° with interplanar distances of 2.92, 2.85, 2.35 and 2.08 Å. The increase in deposition time allows more materials to be deposited onto the substrate and thicker films to be formed.

The scanning electron micrographs (Figure 7) show the morphology of the deposits for the films prepared at 15 and 60 min. The film prepared at 15 minutes shows incomplete coverage of material over the surface of the substrate. As the deposition time was increased films starts to grow thicker as can been seen in the micrograph of the film deposited at 60min.

Figure 8 shows the XRD pattern for the unannealed and annealed samples. The as-deposited sample with a thickness of 28.6 μm shows four peaks and the interplanar distances obtained matches with the standard JCPDS data. The peaks obtained indicate that an orthorhombic SnSe structure with (201), (011), (111) and (410) planes have been deposited. The (111) plane shows the highest intensity peak for the as-deposited and annealed samples. The results obtained from this study reveal interesting information about SnSe.

Comparison between the as-deposited film and the annealed film at 150 °C show that the intensity of the peaks increased indicating greater crystallinity compared to the annealed film. This could be clearly seen in the (111) peak, which is more intense. The number of peaks in the annealed film also increased to five peaks with interplanar distances matching standard values. Annealing at 150 °C improved the crystallinity of the films. As the annealing temperature was increased to 250 °C, the intensity of the peaks shows a decline. The total peaks attributable to SnSe also reduced to three peaks. This clearly indicates that exposure at high temperature decomposes the film. The number of peaks decreased to three and finally two at annealing temperature of 450 °C. The intensity if the (111) plane decreased gradually with increase in the annealing temperature.

Figure 9 shows the SEM micrographs of the as-deposited and annealed sample at 150 °C. The SEM micrograph of the as-deposited shows a distribution of particle, which covers

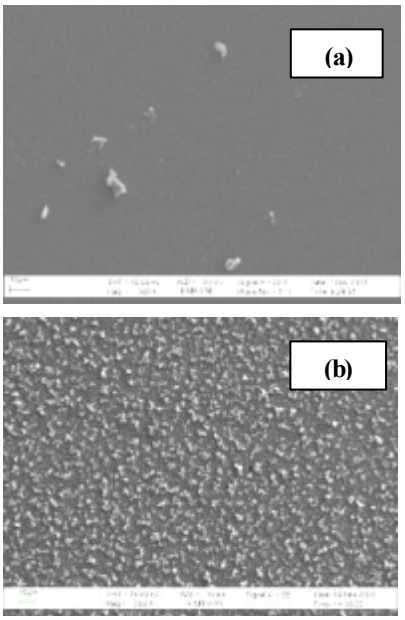

FIGURE 7 SEM micrographs of samples prepared at 15 (a) and 60 (b) min

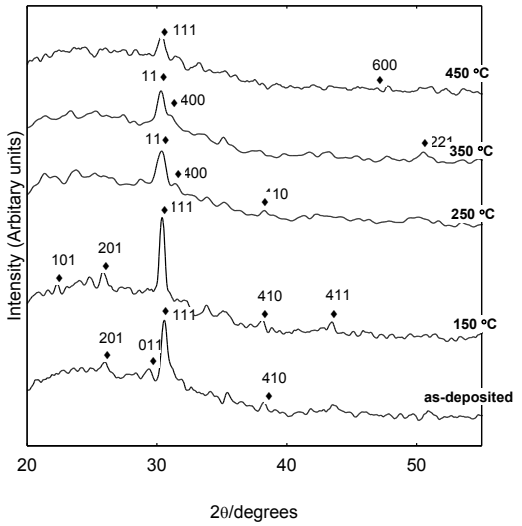

FIGURE 8 X-ray diffraction patterns of the unannealed sample and annealed samples at different temperature

the surface of the substrate completely. No pinholes or cracks could be observed for this sample. The SEM micrograph of the sample annealed at 150 °C shows well-defined particle edges. The grain size increased compared to the untreated sample and shows an agglomerated morphology. The sample appears very homogenous.

From the results it is clearly understood that heat treatment of 250 °C and above have deteriorating effects on SnSe films. Figure 10 shows the difference between the photocurrent

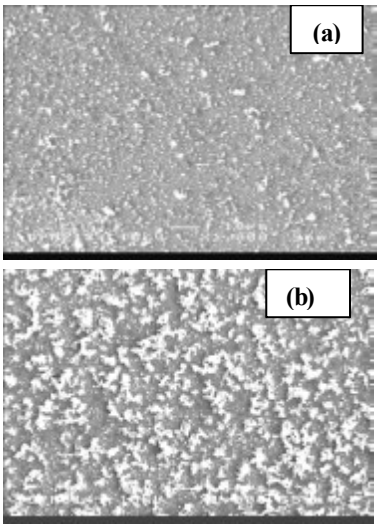

FIGURE 9 SEM micrographs of untreated (a) and annealed at 150 °C (b) samples

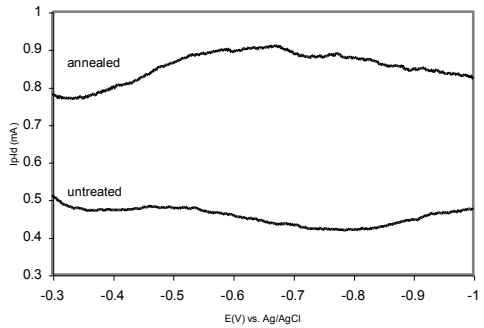

FIGURE 10 Difference between the photocurrent (Ip) and darkcurrent (Id) of the untreated and treated samples (annealed at 150 °C)

(Ip) and darkcurrent (Id) for the as-deposited film and the film annealed at 150 °C. An increase in the current could be observed for both the samples, which was employed as a cathode in the electrochemical cell as the potential is swept into the more negative region. The comparison between the two indicates an increase in the photoresponse. This shows that 150 °C annealing promotes growth of crystallites and thereby reduces the grain boundary areas, which are known to act as recombination centers for minority carriers and trapping centers for majority carriers. This current change with the illumination confirms that the films posses photoconducting behavior. Since the photocurrent occurs on the negative (cathode) potential, the films are of *p*-type (positive) and they can be deployed as a photocathode in a photoelectrochemical cell for reduction reactions.

Acknowledgements

We are grateful to the Malaysian Government for providing the grant under IRPA No. 09-02-04-0369-EA001. The author would like to thank the Ministry of Science, Technology and Innovations for the National Science Fellowship (NSF) award.

References

Agnithothri O.P., Jain A.K., Gupta B.K. (1979) Single crystal growth of stannous selenide. *J. Cryst. Growth* 46: 491-494.

Bennouna A., Tessier P., Priol M., Dang Tran Q., Robin S. (1983) Far Ultraviolet Photoelectric Study of Thin SnSe Evaporated Films. *phys. stat. sol. (b)* 117: 51-56.

Dang Tran Q. (1985) Electrical Properties and Optical Absorption of SnSe Evaporated Thin Films. *phys. stat. sol. (a).* 86: 421-426.

Engelken R.D., Berry A.K., Van Doren T.P., Boone J.L., Shahnazary A. (1986) Electrodeposition and Analysis of Tin Selenide Films. *J. Electrochem. Soc*. 133: 581-585.

Ghazali A., Zainal Z., Hussein M.Z., Kassim A. (1998) Cathodic electrodeposition of SnS in the présence of EDTA in aqueous media. *Sol. Energy Mater. Sol. Cell.* 55 : 237-249.

John J., Pradeep B., Mathai E. (1994) Tin Selenide Thin Films Prepared by Reactive Evaporation. *J. Mater. Sci.* 29: 1581-1583.

Lindgren T., Larsson M., Lindquist S. (2002) Photoelectrochemical characterization of indium nitride and tin nitride in aqueous solution. *Sol. Energy Mater. Sol. Cells* 73: 377-389.

Pramanik P., Bhattacharya S. (1988) Tin Selenide Thin Films Prepared by Chemical Bath Deposition. *J. Mater, Sci. Lett.* 7: 1305-1306.

Pattabi M., Sebastian P.J., Mathew X., Bhattacharya R.N. (2000) Preparation and characterization of copper indium diselenide films by electroless deposition. *Sol. Energy Mater. Sol. Cells* 63: 315-323.

Riveros G., Gomez H., Henriquez R., Schrebler R., Marotti R.E., Dalchiele E.A. (2001) Electrodeposition and characterization of ZnSe semiconductor thin films. *Sol. Energy Mater. Sol. Cell.* 70: 255-268.

Saloniemi H., Kanniainen T., Ritala M., Leskela M., Lappalainen R. (1998) Electrodeposition of Lead Selenide Thin Films. *J. Mater. Chem.* 8: 651-654.

Singh J.P., Bedi R.K. (1991) Electrical properties of flash-evaporated tin selenide films. *Thin Solid Films* 199: 10-12.

Subramanian B., Mahalingam T., Sanjeeviraja C., Jayachandran M., Chockalingam M.J. (1999) Electrodeposition of Sn, Se and the Material Properties of SnSe Films. *Thin Solid Films* 357: 119-124.

Suguna P., Mangalaraj D., Narayandass S.A.K., Meena P. (1996) Structure, Composition, Dielectric, and AC Conduction Studies on Tin Selenide Films. *phys. stat. sol. (a)* 155: 405-416.

Terada T. (1971) Vacuum deposition of tin-selenium films. *J. Phys. D: Appl. Phys.* 4: 1991-1997.

Yu J.G., Yue A.S., Stafsudd J.R. (1981) Growth and electronic properties of SnSe semiconductors. *J. Cryst. Growth* 54: 248-252.

Zweibel K. (2000) Thin Film PV Manufacturing: Materials Costs and Their Optimisation. *Sol. Energy Mater. Sol. Cells* 63: 375-386.